Direct X-Ray Detecting Gap-Type Thin-Film Transistors for Ultra-High Spatial Resolution Flat-Panel Image Receptors

Chi-Hao Lin, Chia-Hsuan Li *, Ya-Hsiang Tai*, Saikiran Khamgaonkar**, Vivek Maheshwari**, Karim Sallaudin Karim***

* Department of Photonics, College of Electrical and Computer Engineering, National Yang Ming Chiao Tung University, Hsinchu, Taiwan, R.O.C.

** Electrical and Computer Engineering, University of Waterloo, Ontario, Canada

Abstract

In this paper, we propose to use Gap-type TFT to implement the direct X-ray detection for ultra-high spatial resolution receptors, which are even suitable for the flexible CT applications. The device test-key is fabricated and measured to show that the X-ray photocurrent of Gap-type TFT is approximate 10 nA large. The preliminary pixel estimation of the direct-readout and passive pixel sensor are presented. This work proves that Gap-type TFT is an extraordinary candidate for the ultra-high spatial resolution direct X-ray detecting system.

Author Keywords

Direct X-ray detector, Gap-type, Thin Film Transistor (TFT), Ultra-High Spatial Resolution, Flat Panel.

1. Introduction

Nowadays, X-ray detector can be generally categorized to indirect-conversion and direct-conversion. Indirect-conversion requires the scintillator to convert the X-ray to visible light. This conversion process and the thickness of scintillator both are the reasons that cause the spatial resolution decrease of detector [1]. Direct conversion detector converts the X-ray directly to the electrical signal, the spatial resolution and detective quantum efficiency can be improved significantly [2]. Due to the challenges such as mass production feasibility, cost and manufacturing complexities, indirect-conversion still dominate the current industry.

Indirect conversion detector usually uses PIN photodiode as the sensor layer to convert the visible light to electrical signal. To achieve enough signal intensity, the photodiode requires relatively large area, which will limit the pixel size and array resolution. The mechanism of amorphous silicon (a-Si) Gap-type thin film transistor (TFT), Light Induced Barrier Lowering (LIBL), gives the potential to shrink the pixel size with high photocurrent [3]. Even Gap-type TFT is used to replace the PIN for the indirect conversion X-ray detector, the spatial resolution can be limited by the oblique light in the scintillator, as shown in Fig. 1.

If the Gap-type TFT can be made to convert the X-ray photons to charge directly, the spatial resolution X-ray flat panel can be greatly improved, as shown in Fig. 2. The first reason is the absence of scintillator, and the second reason is the small are of Gap-type TFT. Furthermore, in the application of CT system shown in Fig. 3, the distance to the X-ray source at the edges of the large area detector can be much longer than that at the center, which makes the X-ray intensity greatly lowered. Using direct detecting Gap-type TFT, the X-ray detecting panel can be formed thin and curve, as shown in Fig. 4, the signal in the edge area of such a large area CT imaging system is excepted much better for its less distance difference.

The proposed large area and curved direct X-ray detecting panel pretty much relies on the key device of direct X-ray detecting (DXD) Gap-Type TFT. In this work, we fabricate the DXD Gap-type TFT and prove that the proposed detector is attainable. In addition, to further push the spatial resolution to the limit, the pixel design is discussed based on the characteristics of the DXD Gap-type TFT.

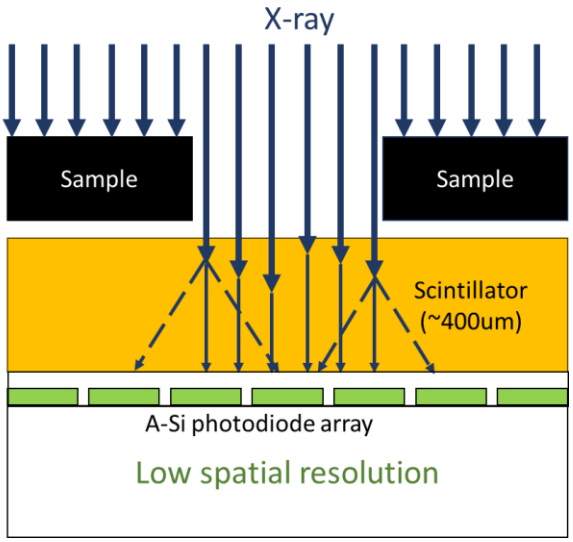

Fig. 1. Illustration of indirect X-ray detector.

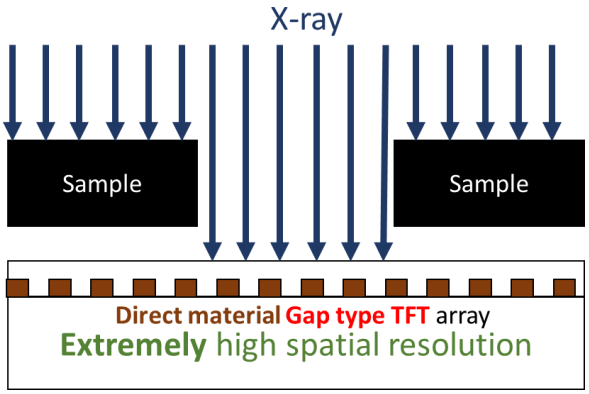

Fig. 2. Illustration of proposed direct X-ray detector.

ISSN 0097-996X/25/5603-1912-$1.00 © 2025

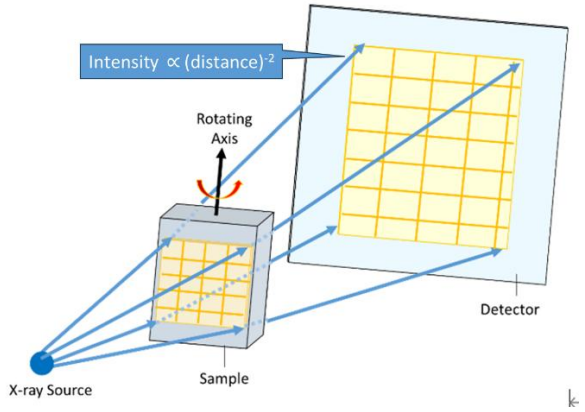

Fig. 3. Illustration of CT system.

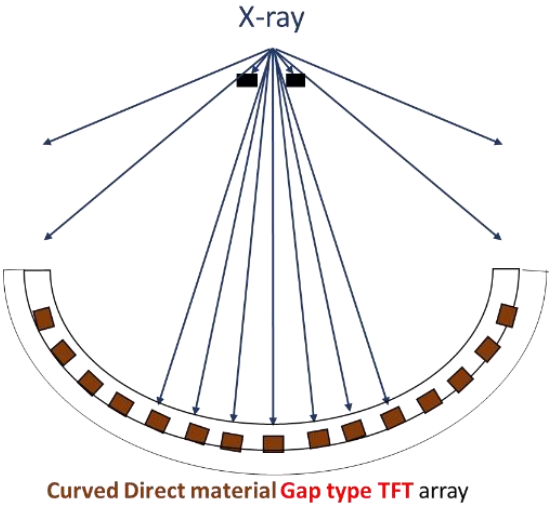

Fig. 4. Proposed large area and curved detector.

2. Device Structure and Fabrication

Fig. 5 shows the schematic illustration of DXD Gap-type TFT. The process is one step away from the control TFT such as a-Si and LTPS. Table 1 lists the layers of materials and the corresponding thickness. The test-key before and after applying the semiconductor are respectively shown in Fig. 6 and Fig. 7. In this work, we use perovskite (MAPbI3) in thickness of 300nm as the direct X-ray detecting semiconductor and spin coating to form the pattern [5].-[7] In real mass production, the thickness can be further adjusted, and the composition of perovskite can be further optimized to obtain larger photocurrent and lower dark current.

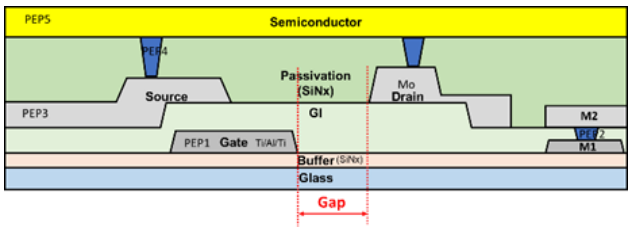

Fig. 5. Schematic illustration of Gap-type TFT

Table 1. Materials and thickness of layers for Gap-type TFT

PEP	Layer	Material	Thickness (nm)
	Buffer	SiNx	300
1	Metal 1	Ti/Al/Ti	50/100/50
2	Contact	SiNx	300
3	Metal 2	Mo	100
4	Passivation	SiNx	150
5	Semiconductor	Perovskite	300

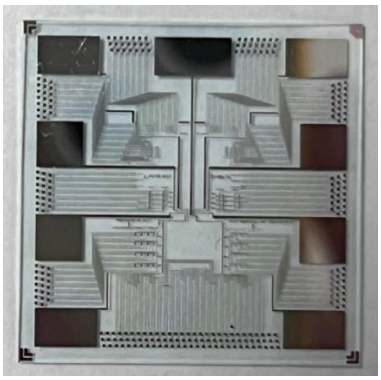

Fig. 6. The image of test-key before depositing perovskite.

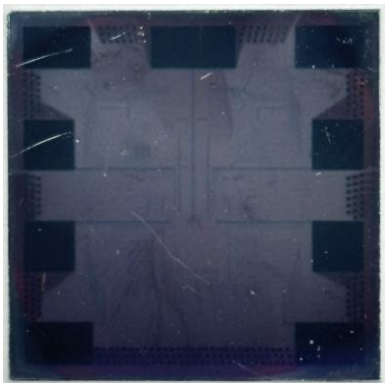

Fig. 7. The image of test-key after depositing perovskite.

3. Device Characteristics

Fig. 8 shows the I_D-V_G of DXD Gap-type TFT under different illumination intensity. The transfer function shows that the X-ray photocurrent is approximate 10 nA under the voltage bias V_{DS}= 5V and V_{GS}= -15V. It proves that the LIBL mechanism is also applicable to X-ray photons in the gap-type structure. Those features and advantages of a-Si Gap-type TFT, such as simple process, high photocurrent level, small area, small parasitic capacitance,…etc., described in [4] are inherent in DXD Gap-type TFT.

Fig. 9 plots the X-ray photocurrent as a function of the applied X-ray dose rate. The DXD Gap-type TFT, with an area of only around 400 μm², features a small size while maintaining high

spatial resolution. The perovskite layer in the device is extremely thin, with a thickness of just 300 nm, contributing to its efficient performance. The operating voltage is within the typical range for standard TFT panels, between ±20 V, and the device generates a photocurrent of approximately 10 nA under X-ray exposure, highlighting its effective response to X-ray radiation at relatively low voltages.

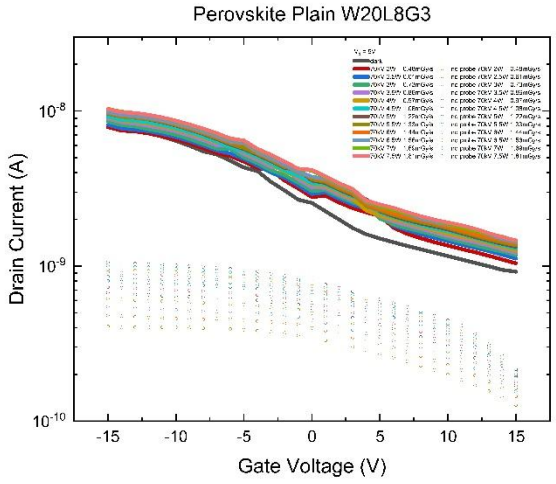

Fig. 8. I_D-V_G curves of DXD Gap-type TFT

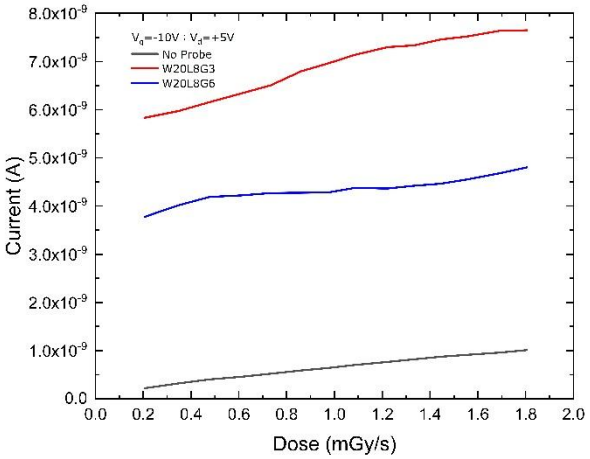

Fig. 9. Photocurrent versus X-ray intensity of Perovskite DXD Gap-type TFT.

4. Sensing Pixel Design

Even though we have the small-area DXD device, we need to consider the sensing pixel design to achieve ultra-high resolution image receptor. Fig. 10 (a) and (b) illustrate passive pixel sensor (PPS) design based on a-Si or IGZO TFT and LTPS TFT, respectively. The similarity and compatibility of the proposed DXD Gap-type TFT and the conventional TFTs give us the benefit to make the pixel as small as possible. Each pixel contains one switch TFT, one sensing TFT, and a capacitor. The capacitor is used to integrate the photocurrent induced by X-ray photons. It can use the next scan line to reset the previous storage charge, but it requires separate Vdd bus line.

Depending on applications, if the photocurrent is large enough, we can directly integrate this photocurrent during the short period of row time, which is called direct readout here. In such operation, the capacitor and the Vdd bus can be omitted to further reduce the pixel size. The corresponding designs for a-Si or IGZO TFT and LTPS TFT are illustrated in Fig. 11 (a) and (b).

In comparison, direct readout design is the most streamlined circuit to realize the finest pixel resolution. According to our evaluation based on 3μm design rule, 900 PPI is achievable with pixel rendering .

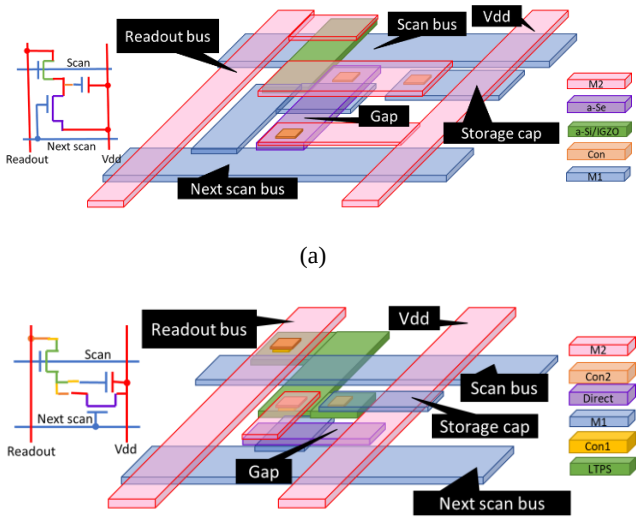

Figure 10. Small passive pixel sensor design for (a) a-Si/IGZO TFT line and (b) LTPS TFT line.

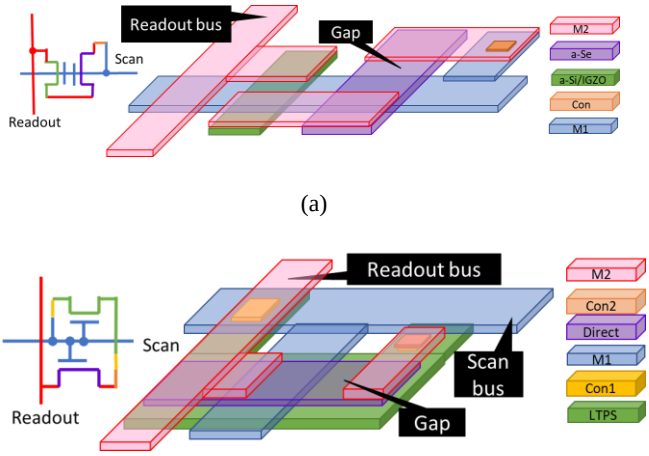

Figure 11. Small direct readout design for (a) a-Si/IGZO TFT line and (b) LTPS TFT line.

5. Conclusion

DXD Gap-type TFT is fabricated and measured. The high photocurrent can be generated directly by X-ray with very small device area. It opens the door to make the large area and curved X-ray image receptors for CT imaging. With the direct-readout pixel design, the pixel pitch of 30μm is obtainable. With process compatible to mature a-Si or LTPS TFT, we believe the ultra-high spatial resolution flat panel image receptors will soon be developed and available in the market.

6. Acknowledgements

This work was supported by the Ministry of Science and Technology under Project number of MOST 111-2926-I-A49-501-G and in part with the Waterloo Institute for nanotechnology, University of Waterloo, Canada.

7. References

1. Y. Xu, Y. Qi, Q. Qian, J. Chen, Z. Yang and K. Wang, "Backside Illuminated 3-D Photosensitive Thin-Film Transistor on a Scintillating Glass Substrate for Indirect-Conversion X-Ray Detection," in IEEE Electron Device Letters, vol. 41, no. 8, pp. 1209-1212, Aug. 2020, doi: 10.1109/LED.2020.3001922.

2. R.R. Karthieka, R. Nafeesa Begum, T. Prakash,, “Direct conversion X-ray sensing nature of bismuth (III) iodide thick films”, Chinese Journal of Physics, Volume 71, 2021, Pages 643-650, ISSN 0577-9073,

3. Y. -H. Tai, C. -C. Tu, Y. -C. Yuan, Y. -J. Chang, P. -C. Wang and Y. -W. Kuo, "The Photosensitive Mechanism of Gap-Type Amorphous Silicon TFT," in IEEE Transactions on Electron Devices, vol. 68, no. 12, pp. 6177-6181, Dec. 2021, doi: 10.1109/TED.2021.3120231.

4. Y. -H. Tai, Y. -C. Yuan, C. -C. Tu and P. -C. Wang, "The Noise Behavior of Gap-Type Amorphous Silicon TFT Under Illumination," in IEEE Journal of the Electron Devices Society, vol. 10, pp. 309-312, 2022, doi: 10.1109/JEDS.2022.3164082.

5. Khamgaonkar, S., Chen, Q., Musselman, K., & Maheshwari, V. (2023). Stable perovskite photocathodes for efficient hydrogen evolution in acidic and basic conditions. Journal of Materials Chemistry A, 11(37), 20079-20088.

6. Khamgaonkar, S. S., Leudjo Taka, A., & Maheshwari, V. Synergistic Passivation of Bulk and Interfacial Defects Improves Efficiency and Stability of Inverted Perovskite Solar Cells. Solar RRL, 2400658.

7. Asgarimoghaddam, H., Khamgaonkar, S. S., Mathur, A., Maheshwari, V., & Musselman, K. P. (2024). Enhancing Internal and External Stability of Perovskite Solar Cells Through Polystyrene Modification of the Perovskite and Rapid Open-Air Deposition of ZnO/AlOx Nanolaminate Encapsulation. Solar RRL, 8(14), 2400111.